
the society for solid-state and electrochemical science and technology

Journal of The Electrochemical Society

Impact of $LiFePO_4$?/?C Composites Porosity on Their Electrochemical Performance

R. Dominko, J. M. Goupil, M. Bele, M. Gaberscek, M. Remskar, D. Hanzel and J. Jamnik

J. Electrochem. Soc. 2005, Volume 152, Issue 5, Pages A858-A863.
doi: 10.1149/1.1872674

Email alerting service Receive free email alerts when new articles cite this article - sign up in the box at the top right corner of the article or click here

To subscribe to *Journal of The Electrochemical Society* go to:
http://jes.ecsdl.org/subscriptions

© 2005 ECS - The Electrochemical Society

Downloaded on 2012-11-11 to IP **138.87.11.21** address. Redistribution subject to ECS license or copyright; see **www.esltbd.org**

Journal of The Electrochemical Society, **152** (5) A858-A863 (2005)
0013-4651/2005/152(5)/A858/6/$7.00 © The Electrochemical Society, Inc.

Impact of $LiFePO_4$/C Composites Porosity on Their Electrochemical Performance

R. Dominko,[a,z] J. M. Goupil,[b] M. Bele,[a] M. Gaberscek,[a,*] M. Remskar,[c] D. Hanzel,[c] and J. Jamnik[a]

[a]*National Institute of Chemistry, SI-1001 Ljubljana, Slovenia*
[b]*ENSICAEN, UMR CNRS 6506, Catalyse and Spectrochimie Lab, F-14050 Caen, France*
[c]*Jozef Stefan Institute, SI-1000 Ljubljana, Slovenia*

Fe(III) citrate was used as a source for synthesis of microsized porous $LiFePO_4$/C particles. All samples, prepared either by solid-state or by sol-gel techniques, are phase-pure triphylite phases, which, however, have different morphology highly influenced by the type of synthesis and synthesis parameters. Their common feature is porosity due to thermal decomposition of citrate anion. The impact of particle porosity on the electrochemical behavior is discussed in terms of qualitative results obtained from scanning electron microscopy (SEM) micrographs and in terms of quantitative results obtained from N_2 adsorption isotherms. The best electrochemical behavior (above 140 mAh/g at C/2 rate during continuous cycling) was obtained with composites prepared at a relatively high heating rate (above 5 K/min). This suggests that interlaced pores were formed inside particles. A strong correlation between the electrochemical results and the heating rate was observed, which could easily be explained based on SEM micrographs and on some trends found in porosity measurements. The latter reveal the main difference between samples prepared by solid-state and by sol-gel techniques.
© 2005 The Electrochemical Society. [DOI: 10.1149/1.1872674] All rights reserved.

Manuscript submitted August 3, 2004; revised manuscript received October 30, 2004. Available electronically March 25, 2005.

There are many materials, which if considered thermodynamically, exhibit high electrical storage capacity but have been found unattractive for industrial applications due to the sluggish charge/discharge kinetics.[1] Certain active materials of interest, such as $LiMPO_4$ or $LiMBO_3$ (M = Fe, Mn, Co, Ni, …),[2-4] exhibit an electron conductivity of 10^{-9} S cm^{-1} or even lower. It has been proposed that in order to achieve high power density, such materials should be prepared and used in a form of nanopowder.[5] It is well known that with particles smaller than 100 nm, it appears to be very difficult to prepare a composite in which each active particle is effectively wired with an electron conductor.[6] Various authors have developed special techniques for preparation of such composites. An effective route is certainly preparation of carbon coatings (paintings) around each active particle.[5,7,8] While serving primarily as an electron conductor, these coatings must also be either porous or very thin to allow easy penetration of lithium ions. The carbon coatings are usually prepared from organic precursors (sugars, polyaromates, etc.) that are added to the reaction mixture before firing, usually in inert or reductive atmosphere. The obtained material is in a form of nanoparticulates and as such, presents potential health, safety, and environmental hazards.[9,10]

Although carbon paintings are crucial for local electron supply to poorly conducting particles such as $LiFePO_4$, they are usually not the only carbon materials in the final electrode formulation. Namely, during electrode preparation a certain amount of carbon black is usually added to create appropriate porosity that allows electrolyte to penetrate across the whole active material. In this way, a situation is created where both lithium cations and electrons are available everywhere on the particle's surface. Although addition of carbon black is essential to obtain a porous composite with good performance, the presence of such electrochemically inactive materials decreases the practical energy and power density of the electrode. In our previous report we showed, however, that it was possible to prepare $LiFePO_4$ particles which already contained considerable internal porosity and where, at the same time, the walls of pores and the outer surface were painted with a nanometer-thick carbon film.[11] Such porous carbon-coated particles offer, at least in principle, two new possibilities: (*i*) less (ideally zero) carbon black additives and/or (*ii*) the use of much larger particles (up to 20 μm large) in electrode preparation.[12]

In the present paper we investigate the role of particles' internal porosity in detail. For this purpose we prepared the $LiFePO_4$ composite materials via a sol-gel route using Fe(III) citrate as a precursor. The particles internal porosity was controlled by appropriate selection of several synthesis parameters, such as the type of synthesis (sol-gel *vs*. solid-state), the heating rate during combustion of precursors, firing time, atmosphere, etc. The obtained porous composites were characterized qualitatively [scanning electron microscopy (SEM) characterization] and quantitatively (porosity measurements). The impact of porosity features on the electrochemical properties of resulting $LiFePO_4$-based cathodes was systematically studied.

Experimental

Several series of $LiFePO_4$/C composites were prepared by a sol-gel method. First, Fe(III) citrate (Aldrich, 22.897–4) was dissolved at 60°C in water. Separately, equimolar water solution of LiH_2PO_4 was prepared from H_3PO_4 (Merck 1.00573) and Li_3PO_4 (Aldrich, 33.889-3). The solutions were mixed together and the obtained transparent sol was dried at 60°C for at least 24 h. After thorough grinding with mortar and pestle, the obtained material was fired in inert (argon) or reductive (5 wt % hydrogen in argon) atmosphere at 700°C for a period of 15 min up to 10 h. The heating rate was between 1 and 100 K/min.

For comparison, additional series of $LiFePO_4$/C composites were prepared by a solid-state technique. The starting materials were similar, with one exception: the concentrated solution of phosphoric acid was replaced with crystallized phosphoric acid (Aldrich 32.027-1). The precursors were ground with mortar and pestle for at least 20 min and fired in a reductive atmosphere at 700°C for 10 h. The heating rate was 5 K/min.

The electrodes were prepared by casting and pressing a mixture of 85 wt % of the as-synthesized material, 7 wt % of a Teflon binder (Aldrich 44,509/6), and 8 wt % of carbon black (Printex XE2, Degussa) on aluminum foil followed by drying in vacuum at 120°C for 24 h. The active material loading was about 5 mg/cm^2 and the typical thickness of the active layer was 50 μm. The electrolyte used was a 1 M solution of $LiPF_6$ in EC:DMC (1:1 ratio by volume), as received from Merck.

A laboratory-made three-electrode test cell was used to carry out the electrochemical tests. The working and the counter (lithium) electrodes were held apart with two separators (Celgard 2402) between which a thin strip of lithium serving as a reference electrode was positioned. The cells were assembled in an argon-filled glove box at room temperature.

* Electrochemical Society Active Member.
z E-mail: Robert.Dominko@ki.si

Downloaded on 2012-11-11 to IP 138.87.11.21 address. Redistribution subject to ECS license or copyright; see www.esltbd.org

Charge-discharge curves were recorded using an EG&G 283 potentiostat/galvanostat at room temperature. The constant current during cell cycling was set to a value between 8.5 and 3400 mA/g (corresponding roughly to C/20 and 20C, respectively). The geometric surface area of the working electrode was always 0.5 cm^2.

X-ray powder diffraction (XRD) patterns were measured on a Philips diffractometer PW 1710 using CuKα radiation in 0.04° 2θ steps from 15 to 90°. Calculations of the unit cell parameters and the XRD profile patterns were performed using a TOPAS R 2.1 software.[13] ^{57}Fe Mössbauer experiments were performed at room temperature using a constant acceleration spectrometer. The source was ^{57}Co in a Rh matrix. Velocity calibration and isomer shifts (IS) are quoted relative to an absorber of metallic iron at room temperature. Experiments were performed both in transmission and scattering geometry. Conversion electron Mössbauer measurements in a He/CH_4 gas flow proportional counter[14] were performed in order to find differences in the depth distribution of Fe cations between the surface of the samples and the bulk. Parameter fits were performed using a standard least-squares fitting routine with Lorentzian lines.

Thermogravimetric analyses (TGA) were performed on a SDT 2960 simultaneous thermal analyzer (TA Instruments, USA). After 15 min equilibration at 25 °C, the temperature was raised at 10 K/min up to 700 °C. The analyses were performed in airflow. The mass loss in the temperature range between 380 and 480°C was taken as a ratio of organic phase in the $LiFePO_4$/C composite.

The textural properties were studied in the macroporous range by transmission electron microscopy (TEM) equipped with electron diffraction (Phillips EM 301) and scanning electron microscopy (SEM –JEOL 5500 LV). Properties of porous system in the 4–200 nm range were determined by nitrogen adsorption at 77 K using an ASAP 2000 instrument from Micromeritics. A sample of mass around 200 mg was loosely pressed into a wafer and then evacuated at 573 K under 0.1 Pa prior adsorption.

Results and Discussion

Physical properties.—All $LiFePO_4$/C composites, prepared either by the sol-gel or the solid-state synthesis, were phase-pure according to their XRD patterns. This one was fully indexed in the space group *Pmna* with cell parameters a = 10.3333 Å, b = 6.0132 Å, and c = 4.6981 Å (Fig. 1a). In as-prepared $LiFePO_4$/C composites we found approximately 2 atom % Fe(III) impurities using a Mössbauer spectroscopy analysis (Fig. 1b).[11] The amount of carbon in the $LiFePO_4$/C composites depended on the atmosphere used in the process of firing, but in all cases, it was lower than calculated theoretically (18 wt %) based on the initial content of citrate, the single source of carbon. Hence, in a reducing atmosphere (5 wt % H_2 in argon), the content of carbon in the $LiFePO_4$/C composites determined by TGA was 5.8 wt %, while in the inert atmosphere (pure argon) the content of carbon was 3.2 wt %.

Besides serving as a source of electronically conducting carbon, it appears that the citrate anion plays a critical role in the formation of structural and micro/nanostructural characteristics of the resulting $LiFePO_4$/C composites. It was already shown in a previous report that the presence of citrate anion led to formation of a peculiar, but electrochemically favorable material's architecture: spongeous, carbon-decorated $LiFePO_4$/C composite, where $LiFePO_4$ had a form of micrometer-sized particles with hierarchical pore size distribution (in micro-, meso-, and macropore ranges).[12] Both the thin carbon film covering all the material's surfaces and the pores are essential for the electrochemical activity of $LiFePO_4$: while the carbon film serves as an electron conductor, the pores, when filled with liquid electrolyte, serve as a source of Li^+ ions. In such a configuration, it is actually the average distance between the pores that determines the length of chemical diffusion paths within the solid skeleton of $LiFePO_4$, the critical transport step, which affects the polarization and the power of insertion electrodes. Here we show that the material's porosity in the proposed citrate-based sol-gel route can be controlled by various experimental parameters, the most important

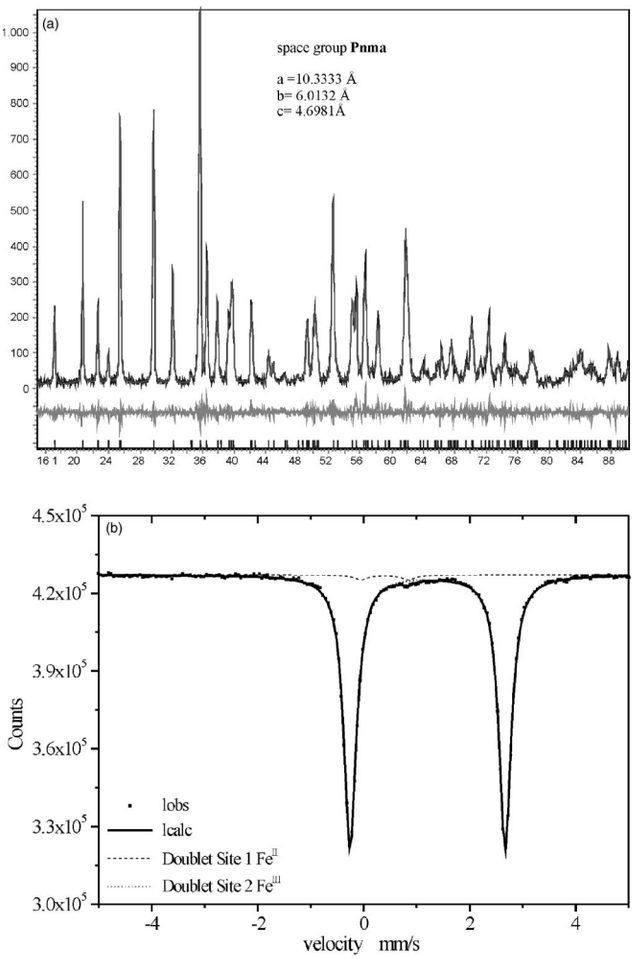

Figure 1. Typical (a) XRD pattern and (b) Mössbauer spectrum recorded at room temperature of $LiFePO_4$-based composites prepared from Fe(III) citrate.

of which seems to be the heating rate (or, alternatively, the time needed to achieve firing temperature), the firing time, the sol-gel concentration, the xerogel aging, and last but not least, the type of synthesis.

SEM characterization was used for qualitative characterization of material morphology. The micrographs in Fig. 2a-c show three different batches of $LiFePO_4$/C composites that were prepared from the same starting xerogel but were fired with different heating rates. The slowest heating rate of 1 K/min (Fig. 2a) yielded composites with, apparently, no apertures on the rough surface (Fig. 2a, upper micrograph). Only careful analysis of many spots on the particles' surface reveals a limited number of small openings, pores that end at the particle surface (Fig. 2a, lower micrograph). However, the surface texture does not necessarily reflect the situation in the bulk material (particle's interior). Indeed, crushing the material into smaller particles reveals significant porosity of the material's interior (Fig. 3). At higher heating rates, the surface of $LiFePO_4$/C composites becomes increasingly more open. At a heating rate of 5 K/min (Fig. 2b), the surface apertures are observable already at low magnification (Fig. 2b, upper micrograph). A closer view shows the presence of numerous small submicrometer apertures (Fig. 2b, lower micrograph), suggesting that the interior pore system is more interlaced if compared with the one described previously. Having in mind this observation it is expected that especially at higher C-rates, these samples will have much better electrochemical behavior than the ones obtained with lower heating rates. To study the effect of

Downloaded on 2012-11-11 to IP 138.87.11.21 address. Redistribution subject to ECS license or copyright; see www.esltbd.org

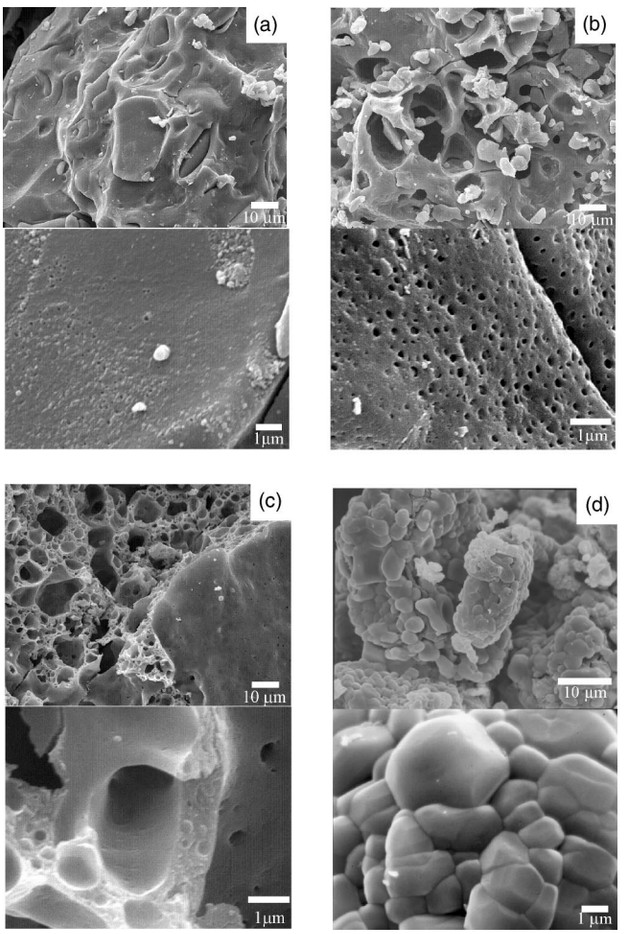

Figure 2. SEM micrographs of $LiFePO_4$/C composites prepared with (a) sol-gel technique using a heating rate of 1 K/min; (b) sol-gel technique using a heating rate of 5 K/min; (c) sol-gel technique using a heating rate 100 K/min, and (d) solid-state technique using a heating rate of 5 K/min.

fast heating rate we put the sample into a preheated oven maintained at a constant temperature of 700 °C. The time needed for the sample to reach the temperature of the oven was about 7 min, so the average heating rate was about 100 K/min. SEM micrographs reveal that several $LiFePO_4$/C particles were broken, probably due to formation of large quantity of gases during citrate anion degradation (Fig. 2c). In fact, in this case the material's architecture on the surface was the same as that observed in the material's interior. Such a structure should present no obstacles to transport of lithium ions from the electrolyte into the material's interior.

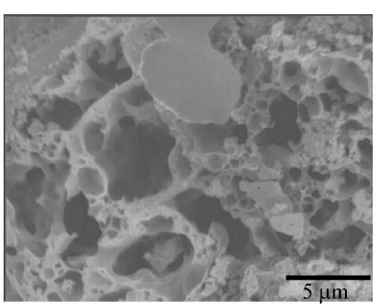

Figure 3. SEM micrograph of a $LiFePO_4$/C composite particle interior with large voids and interlaced pore system.

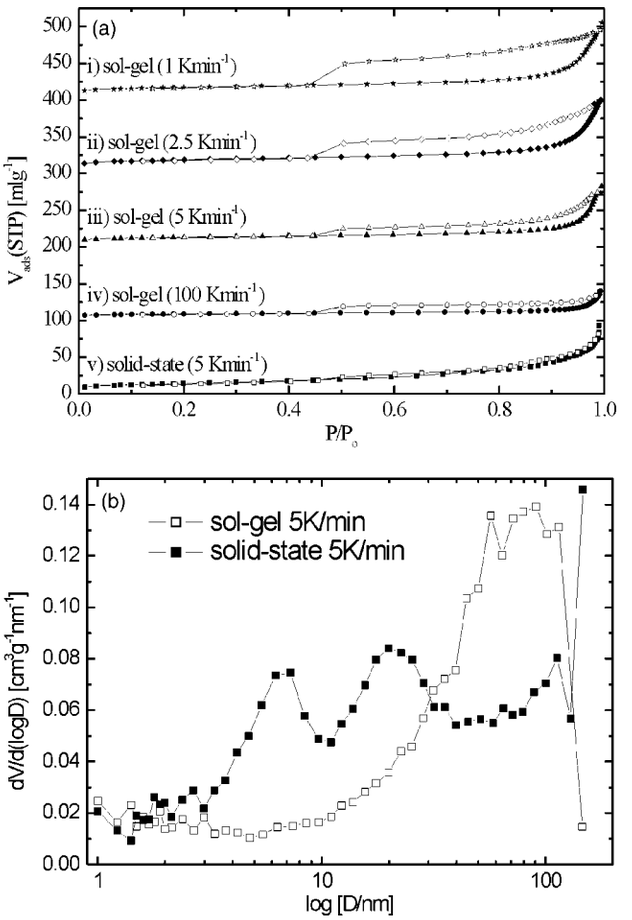

Figure 4. (a) N_2 adsorption isotherms of $LiFePO_4$/C composites prepared either by sol-gel or solid-state techniques using different heating rates: (*i*) sol-gel, heating rate 1 K/min; (*ii*) sol-gel, heating rate 2.5 K/min; (*iii*) sol-gel, heating rate 5 K/min; (*iv*) sol-gel, heating rate 100 K/min, and (*v*) solid-state, heating rate 5 K/min. Full symbol corresponds to the adsorption branch and empty symbol to the desorption branch. For the sake of readability the isotherms are shifted upward for $n \times 100$ mL g^{-1}. (b) BJH distribution of pores from adsorption branch.

For comparison, we also prepared $LiFePO_4$/C composites from Fe(III) citrate using a solid–state synthesis route. Figure 2d shows the resulting material when the heating rate was 5 K/min. The microsized particles, which have an appearance typical of conglomerate of smooth single crystals, do not exhibit any apertures on the surface, even at larger magnifications (Fig. 2d lower micrograph). However, crushing this material into smaller particles reveals a similar porous structure as in the case of sol-gel prepared composites (Fig. 3).

A more quantitative analysis of possible differences between the $LiFePO_4$/C composites mentioned previously was obtained by measurements of N_2 adsorption isotherms. An obvious difference has been observed comparing the composites prepared by sol-gel technique with the ones prepared by the solid–state route. The N_2 isotherms shown in Fig. 4 belong to type IV, lacking for a clear plateau at saturation, whatever the material. Such isotherms are characteristic of solids with a wide distribution of pores, which invades in the macroporous range. The isotherms of samples synthesized by the sol-gel technique show a large, flat H3 hysteresis loop, abruptly closing at P/P° about 0.42, which reveals the emptying of pores with small apertures to the intergranular void space.[15] Moreover, analysis of the low-pressure part of the isotherm reveals micropores (see

Downloaded on 2012-11-11 to IP 138.87.11.21 address. Redistribution subject to ECS license or copyright; see www.esltbd.org

Table I. Porosity measurements–N_2 isotherm results.

Model		HH t-plot					BJH ads	
Synthesis technique	Heating rate (K/min)	V_{pore} (mL g^{-1})	V_{mic} (mL g^{-1})	$S_{t\text{-}plot}$(m^2 g^{-1})	V_{meso} (mL g^{-1})	$V_{restricted}$ (mL g^{-1})	S_{ext} (m^2 g^{-1})	Pore size (nm)
Sol-gel	1	0.096	0.016	24	0.07	0.044	26	60
Sol-gel	2.5	0.094	0.018	26	0.066	0.029	35	40-60
Sol-gel	5	0.062	0.013	18	0.042	0.014	25	90
Sol-gel	100	0.029	0.010	9	0.019	0.013	12	70
Solid-state	5	0.088	0.002	45	0.088	0.002	44	7 and 20

Table I). In contrast, samples prepared via the solid-state route show an isotherm with thin hysteresis loop, almost without any presence of micropores.

A model of the porous system was constructed as a collection of cylindrical pores closed at one end (in accordance with the micrographs) using the BJH algorithm.[16] From the adsorption branch, the pore size distribution of the inner part of these pores was delineated. According to the H3 loop, the information contained in the desorption branch is dominated by a false maximum in pore size distribution located at 2 nm, confirming the presence of restricted apertures to the void space. Detailed analysis of N_2 isotherms is given in Table I.

The figures magnify the difference between the materials obtained by the solid-state route and the sol-gel route. While the latter materials exhibit significant microporosity, the micropore volume of the former is reduced from about 0.02 to 0.002 mL g^{-1}. Furthermore, its pore size distribution (in the range from 4 nm to 200 nm) appears bimodal in contrast to the wider one, centered at about 60 nm, exhibited by the sol-gel samples. For comparison, BJH pore size distribution derived from the adsorption branch of the isotherm is shown in Fig. 4b. Although the differences in figures obtained for sol-gel samples heated at different rates are not so pronounced; some conclusions are possible also in that case. The microporosity observed in samples prepared with the sol-gel technique has its origin in the carbon layer (it disappears with the burning out of the carbon deposit), and it is strongly correlated with the amount of carbon in the composite, irrespective of being prepared in a reductive or in an inert atmosphere. We need to stress that the microporosity observed in such composites is due to the more homogenous xerogel composition (homogeneous on molecular level) if compared with the precursor mixture for solid-state synthesis.

Porosity measurements have given us a clear indication that the heating rate has a limited but measurable influence on the porosity. Comparing the parameters given in Table I the following conclusion can be drawn. At a moderate heating rate, the volumes due to micropores and mesopores (pores with a diameter smaller than 50 nm) are held nearly constant, V_{mic} = 0.02 mL g^{-1} and V_{meso} = 0.07 mL g^{-1}, but the pore size restrictions leading to the $V_{restricted}$ = 0.044 mL g^{-1} occur at low heating rate. At faster heating rate that is above about 5 K min^{-1}, a significant but smaller microporous volume is obtained but the open surface and the mesoporous volume begin to drastically decrease.

This observation agrees with the description of the materials obtained from SEM micrographs, namely, that larger macropores are formed due to a more rapid gas evolution at a higher heating rate. However, this is not necessarily connected neither with the number of meso- and macropores nor with their interlacement. Namely, observation of numerous apertures on the particle's surface of materials prepared with a higher heating rate leads to a conclusion that the pores are more interlaced. At least, numerous apertures on the surface enable electrolyte penetration into the particle interior. This is especially important if pores have restrictions (N_2 isotherm hystereses suggest such "ink-bottle" shape of pores). Interestingly, S_{tplot} area, which measures the extent of the area, constructed at the exterior of the micropores (in meso- and macropores), shows a significant difference between the solid–state and the sol-gel samples (Table I, column 5). Also measurable, but smaller, difference has been observed within sol–gel samples obtained from different xerogels (that is, prepared from sols with different concentrations). Open surface is revealed both by more apertures captured by the SEM pictures and the high S_{tplot} obtained from N_2 isotherms. Based on numerous characterizations, we can make a rather general conclusion that besides the heating rate, parameters like the technique of preparation, the gel concentration, the xerogel aging, and the amount of carbon in $LiFePO_4$/C composite also affect porosity of the final composite.

Electrochemical properties.—Typical charge and discharge curves of the sol–gel prepared material obtained at a heating rate of 5 K/min are shown in Fig. 5. The reversible capacity at "C/20" is approximately 160 mAh/g (the mass taken into account is the inorganic part of the $LiFePO_4$/C composite obtained from TGA; excluding the remaining Fe^{3+} in the composite would give even a higher value). Comparison of the electrochemical performance of this material with the performance of other materials previously discussed in terms of their microstructures is shown in Fig. 6. The best results at high rates (5C or approximately 850 mA/g) are similar to the best results obtained in literature (120 mAh/g) using other preparation procedures,[5,8,17] but it is worth pointing out that the slope of the capacity-rate curve is somewhat less steep in our case. Consistently with expectations based on SEM observations and porosity measurements, we can see that particles with more apertures on the surface gave better electrochemical performance. In fact, the surface obtained at the heating rate of 5 K/min is already "open" enough or the particle's interior is successfully interlaced with a pores system, which allowed unhindered transport of electrolyte into the particle's interior, so further increase in the heating rate does not affect the electrochemistry (the curve for 100 K/min is within experimental

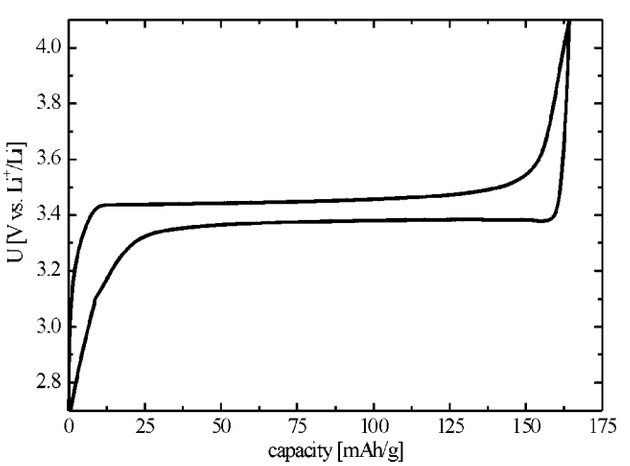

Figure 5. Discharge-charge curve of $LiFePO_4$/C composite in the 2nd cycle at a current density of 8.5 mAh/g (C/20 rate). A composite prepared by sol-gel with a heating rate of 5 K/min was used for the measurement.

Downloaded on 2012-11-11 to IP 138.87.11.21 address. Redistribution subject to ECS license or copyright; see www.esltbd.org

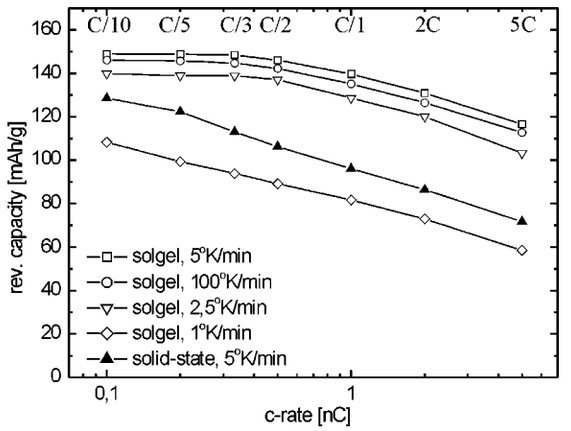

Figure 6. Rate capability of composites prepared at different heating rates. The cell was first charged with a current density of 34 mA/g (C/5) to 4.1 V *vs.* lithium reference electrode and then additionally discharged with a current density of 8.5 mA/g (C/20) to 4.1 V, before it was discharged to 2.7 V with the current densities given in the graph, that is, from 17 mA/g to 850 mA/g (C/10 to 5C rates). The composites were prepared by a sol-gel or a solid-state technique as described in the Experimental section. The firing time was 10 h.

error equal to that for 5 K/min). As expected, the solid-state-synthesis derived sample shows the poorest behavior.

Figure 7 shows stability of the prepared samples during continuous cycling at a current density of 85 mA/g (C/2 rate). Note that some sol-gel samples show improved behavior after a certain number of cycles while the performance of others remains unchanged or even decreases. Again, it is possible to correlate this feature with the number of apertures on the particle's surface of the prepared samples. The more open the surface of a given sample, the more will the performance improves with cycling. With a more interlaced pore system (obtained at higher heating rates), the reason for gradual improvement of capacity might be a slow penetration of electrolyte into all openings and/or formation of cracks in the carbon layer that enables further electrolyte penetration. More likely both phenomena contribute to gradual capacity improvement during continued cycling. A similar improvement of capacity with cycling has also been observed in literature[5,18] but in the case of powderized rather than inherently porous samples. In Fig. 8 we compare the behavior of

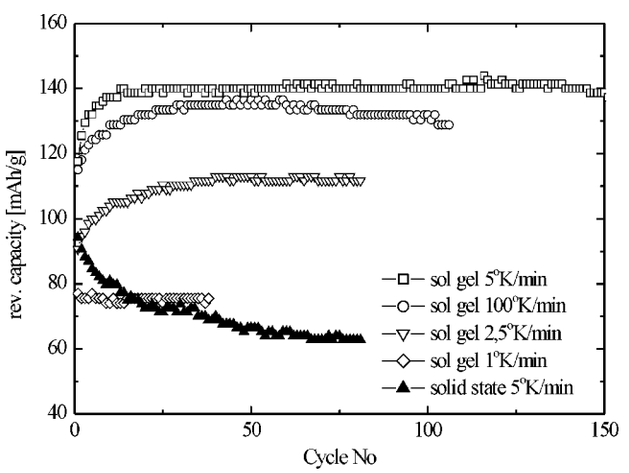

Figure 7. Impact of heating rate on the reversible capacity obtained at C/2 rate (the cell was both charged and discharged at this rate). The symbols denote the same conditions as in Fig. 6.

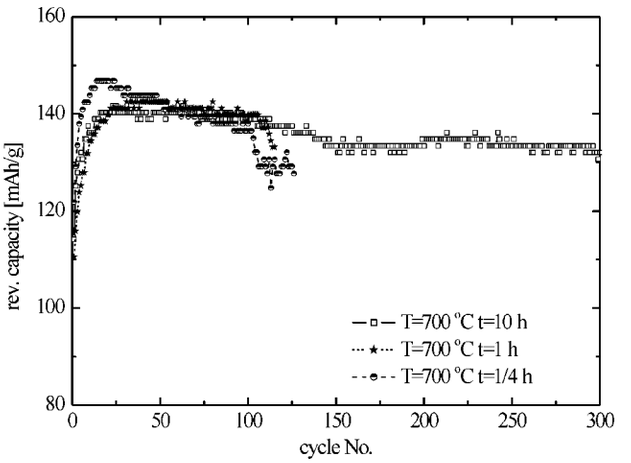

Figure 8. Reversible capacity obtained at C/2 rate (the cell was both charged and discharged at this rate). The composites were prepared by sol-gel with a heating rate of 5 K/min.

$LiFePO_4$/C composites obtained by sol-gel synthesis at a heating rate of 5 K/min, but with different firing times at the temperature of 700°C. The cycling stability at the current density of 85 mA/g (C/2) is not affected significantly by the firing time.

The results shown are in accordance with the basic hypothesis, *i.e.*, that the electrochemical kinetics of $LiFePO_4$–based composites can be fast as long as the solid–state diffusion paths for lithium are short enough and the materials surface is coated with an electron conductor. Apart from carbon–coated nanoparticulate materials,[7,8,19] porous carbon-coated materials also satisfy these criteria. The porous systems can be considered as an inverse picture of the nanoparticulate systems, where the active nanoparticles are replaced by micrometer to nanometer-sized pores. The voids between the nanoparticles are replaced by solid active material, while interphase between the pores and solid material is in both cases occupied by an electron-conducting carbonaceous layer. At least theoretically, such an inverse composite structure can have two major advantages: (*i*) there is no nanoparticulate solid material present, which makes preparation of the electrode composite easier while at the same time avoiding the problem of potential health, safety, and environmental hazard,[9,10] and (*ii*) with careful selection of precursors it seems to be easier to control the length of solid diffusion paths by controlling the material's porosity than to control the size distribution of solid particles, especially when reducing the sizes below 100 nm.

Conclusions

The synthesis of $LiFePO_4$ based on Fe(III) citrate yields inherently porous $LiFePO_4$/C composite materials, regardless of whether the synthesis route is sol-gel or solid-state reaction based. However, SEM characterization and porosity measurements show some pronounced morphological differences, which are likely the reason for the different electrochemical behavior. SEM characterization shows that particles prepared by solid-state reaction do not have any apertures on the surface, while apertures of various magnitutes are easily found on the particles prepared from xerogel. Unlike the sol-gel procedure, the solid-state technique gives a material with negligible volume of micropores. In the solid-state-derived samples, smaller pores are constructed in the 4 - 200 nm range. The absence or a negligibly small number of surface apertures is reflected already at low C-rates, where the solid-state derived samples give a maximum capacity of ca. 130 mAh. We speculate that at higher rates the average diameter of pores also plays an important role, namely, it determines the rate of Li ion supply[20] to the active material. So, the performance of solid-state-derived material is additionally suppressed.

Downloaded on 2012-11-11 to IP 138.87.11.21 address. Redistribution subject to ECS license or copyright; see www.esltbd.org

Within the same technique (sol-gel) the increase in heating rate leads to a larger number of surface apertures, a smaller mesoporous volume, and a more interlaced pore system, while the micropore volume does not change significantly. These features lead to a better electrochemical rate performance.

The present composites were not optimized in terms of the highest possible energy density but rather in terms of fast electrochemical kinetics. Preliminary results show that similar architecture with significantly improved electrochemical kinetics is also possible with other polyanionic compounds, such as $LiMnPO_4$,[21] $LiMnBO_3$, and $LiFeBO_3$.

Acknowledgment

Financial support from the Ministry of Education, Science and Sport of Slovenia is fully acknowledged.

The National Institute of Chemistry, Slovenia, assisted in meeting the publication costs of this article.

References

1. J.-M. Tarascon and M. Armand, *Nature (London)*, **414**, 359 (2001).
2. A. K. Padhi, K. S. Nanjundaswamy, C. Masquelier, S. Okada, and J. B. Goodenough, *J. Electrochem. Soc.*, **144**, 1609 (1997).
3. A. Yamada and S.-C Chung, *J. Electrochem. Soc.*, **148**, A960 (2001).
4. V. Legagneur, Y. An, A. Mosbach, R. Portal, A. Le Gal La Salle, A. Verbaere, D. Guyomard, and Y. Piffard, *Solid State Ionics*, **139**, 37 (2001).
5. H. Huang, S.-C. Yin, and L. F. Nazar, *Electrochem. Solid-State Lett.*, **4**, A170 (2001).
6. R. Dominko, M. Gaberscek, J. Drofenik, M. Bele, S. Pejovnik, and J. Jamnik, *J. Power Sources*, **119-121**, 770 (2003).
7. N. Ravet, J. B. Goodenough, S. Besner, M. Simoneau, P. Hovington, and M. Armand, Abstract 127, The Electrochemical Society and The Electrochemical Society of Japan Meeting Abstracts, Vol. 99-2, Honolulu, HI, Oct 17-22, 1999.
8. Z. Chen and J. R. Dahn, *J. Electrochem. Soc.*, **149**, A1184 (2002).
9. R. F. Service, *Science*, **300**, 243 (2003).
10. G. Brumfiel, *Nature (London)*, **424**, 246 (2003).
11. R. Dominko, M. Gaberscek, M. Bele, M. Remskar, D. Hanzel, S. Pejovnik, and J. Jamnik, *J. Electrochem. Soc.*, **152**, A607 (2005).
12. M. Gaberscek, R. Dominko, M. Bele, M. Remskar, D. Hanzel, and J. Jamnik, *Solid State Ionics*, To be published.
13. Bruker AXS (2003): *TOPAS V2.1: General Profile and Structure Analysis Software for Powder Diffraction Data*, User's Manual, Bruker AXS, Karlsruhe, Germany (2003).
14. D. Hanžel, P. Griesbach, W. Meisel, and P. C. Gutlich, *Hyperfine Interact.*, **71**, 1441 (1992).
15. *Adsorption, Surface Area, and Porosity*, 2nd ed., S. J. Gregg, and K. S. W. Sing, Editors, Academic Press, New York (1982).
16. E. P. Barrett, L. G. Joyner, and P. P. Halenda, *J. Am. Chem. Soc.*, **73**, 373 (1951).
17. S.-Y. Chung, J. T. Bloking, and Y.-M. Chiang, *Nat. Mater.*, **1**, 123 (2002).
18. S. Franger, F. La Cras, C. Bourbon, and H. Rouault, *J. Power Sources*, **119-121**, 252 (2003).
19. J. Barker, M. Y. Saidi, and J. L. Swoyer, *Electrochem. Solid-State Lett.*, **4**, A170 (2001).
20. S. Anderson and J. O. Thomas, *J. Power Sources*, **97-98**, 498 (2001).
21. D. Arcon, A. Zorko, R. Dominko, and Z. Jaglicic, *J. Phys.: Condens. Matter*, **16**, 5531 (2004).

Downloaded on 2012-11-11 to IP 138.87.11.21 address. Redistribution subject to ECS license or copyright; see www.esltbd.org